

Comparison of GRCo-84 to Other Cu Alloys With High Thermal Conductivities

Henry C. de Groh III,¹ David L. Ellis,¹ and William S. Loewenthal²

¹NASA Glenn Research Center, 21000 Brookpark Road, Cleveland, OH 44135

²Ohio Aerospace Institute, 21000 Brookpark Road, Cleveland, OH 44135

The mechanical properties of six highly conductive copper alloys, GRCo-84, AMZIRC, GlidCo Al-15, Cu-1Cr-0.1Zr, Cu-0.9Cr, and NARloy-Z were compared. Tests were done on as-received hard drawn material, and after a heat treatment designed to simulate a brazing operation at 935 °C. In the as-received condition AMZIRC, GlidCo Al-15, Cu-1Cr-0.1Zr and Cu-0.9Cr had excellent strengths at temperatures below 500 °C. However, the brazing heat treatment substantially decreased the mechanical properties of AMZIRC, Cu-1Cr-0.1Zr, Cu-0.9Cr, and NARloy-Z. The properties of GlidCo Al-15 and GRCo-84 were not significantly affected by the heat treatment. Thus there appear to be advantages to GRCo-84 over AMZIRC, Cu-1Cr-0.1Zr, Cu-0.9Cr, and NARloy-Z if use or processing temperatures greater than 500 °C are expected. Ductility was lowest in GlidCo Al-15 and Cu-0.9Cr; reduction in area was particularly low in GlidCo Al-15 above 500 °C, and as-received Cu-0.9Cr was brittle between 500 and 650 °C. Tensile creep tests were done at 500 and 650 °C; the creep properties of GRCo-84 were superior to those of brazed AMZIRC, Cu-1Cr-0.1Zr, Cu-0.9Cr, and NARloy-Z. In the brazed condition, GRCo-84 was superior to the other alloys due to its greater strength and creep resistance (compared to AMZIRC, Cu-1Cr-0.1Zr, Cu-0.9Cr, and NARloy-Z) and ductility (compared to GlidCo Al-15).

Keywords GRCo-84, AMZIRC, GlidCo Al-15, Cu-Cr-Zr, Cu-Cr, NARloy-Z, Copper, compression, tension, creep, mechanical properties

Introduction

GRCo-84 (Cu-8 at%Cr-4 at% Nb) is a newly-developed copper alloy with an attractive balance of high temperature strength, creep resistance, low cycle fatigue life, and thermal conductivity. Our goal is to compare GRCo-84 to similar commercial copper alloys in a consistent manner. Data on alloys such as NARloy-Z, AMZIRC, GlidCo Al-15 low oxygen grade, Cu-0.9Cr, and Cu-1Cr-0.1Zr can be found in the literature.^[1-15] However, the test conditions are rarely matching for “apples-to-apples” comparisons. Most literature also deals only with as-received material. The alloys being considered in this work are used in high temperature applications where high thermal conductivity, high strength, and resistance to creep and low cycle fatigue are required. Such applications include high performance metal gaskets, rocket engine combustion chambers, nozzle liners, and various Reusable Launch Vehicle (RLV) technologies.^[1] In regeneratively cooled combustion chamber applications, such as nozzle liners, these alloys are subjected to the combustion gas temperatures on the hot side and are cooled by cryogenic hydrogen flow on the back side. The tensile, creep, low cycle fatigue, and compressive strength of GRCo-84 will be compared to those of the existing commercially available alloys shown in Table 1. To compare the properties these alloys would actually have during use, they were tested in the as-received condition and after a heat treatment designed to simulate a typical high temperature brazing cycle often needed in the manufacturing process.^[2] The selected brazing heat treatment cycle is presented in Table 2.

GRCo-84 is a dispersion and precipitation hardened alloy made using rapid solidification and powder metallurgical techniques. Consolidation is accomplished by hot isostatic pressing (HIP) or direct extrusion. After consolidation most processing methods used with high strength copper alloys can be used to form GRCo-84, e.g., hot and cold rolling. The solubilities of Cr and Nb are very high in liquid copper but very low in solid Cu. Chromium and Nb have a high affinity for each other, thus nearly all of the Cr and Nb combine to form the hardening intermetallic phase Cr₂Nb. This leaves a nearly pure Cu matrix. The high purity of the copper matrix leads to a thermal conductivity for the alloy that is 72 to 82% of that of pure oxygen-free Cu.^[3]

AMZIRC can be cast as well as produced using powder metallurgy. Peak strengths in AMZIRC are achieved through cold work combined with precipitation hardening and are lost if the hardened material is exposed to a high temperature braze cycle or if fully annealed.^[4] Approximately 80% of the strength gains normally achieved in AMZIRC are due to cold work, with only modest additional gains achieved upon aging.^[5] Horn and Lewis found that cold-worked AMZIRC retains much of its strength up to about 500 °C without becoming brittle. They also noted that the excellent strength of heavily worked rod was not achieved in their billets and that there was an inability to obtain uniform hardening in large billets.^[6] AMZIRC’s low cycle fatigue properties have been reported by Conway et al.^[7] and by Hannum et al.^[8] and property reviews which have included AMZIRC have been

published.^[5,9] Dalder et al. found the room temperature ultimate tensile strength of AMZIRC to be about 430 MPa and that AMZIRC's room temperature strength dropped to 241 MPa after exposure to >500 °C.^[10] The room temperature ductility of AMZIRC decreases with cold work, with elongation at failure going from about 50% for unworked material to 10%^[5] or lower^[10] for material worked >30%. AMZIRC has a solution temperature near 910 °C and aging temperatures near 525 °C for unworked material, and 425 °C for cold worked material.

GlidCop Al-15 is dispersion hardened with very fine Al₂O₃ particles. Considerable research has been published on GlidCop Al-15. Dalder et al.^[10] found GlidCop more thermally stable than AMZIRC. Wycliffe^[5] found (in 1984) that the only copper alloys with good strength above 650 °C were oxide dispersion strengthened (ODS) alloys such as GlidCop. However, Wycliffe also noted that the ductility and low cycle fatigue properties of ODS copper alloys at elevated temperatures were poor. Stephens and Schmale showed that heat treat cycles which simulate brazing operations as high as 980 °C result in only a small decline in ultimate tensile strength (~13%) in GlidCop Al-15, and that ductility improves substantially.^[2] Stephens et al.^[11] showed that fine-grained GlidCop Al-15 that was annealed for 15 minutes at 980 °C was stronger in room temperature tension than coarse-grained GlidCop Al-15 annealed 100 hr. at 980 °C, but that as the test temperature increased, the advantage fine-grained GlidCop Al-15 had vanished, until at 800 °C coarse-grained GlidCop Al-15 was stronger than fine-grained GlidCop Al-15. In work due to Conway et al. the ductility and low-cycle-fatigue properties of GlidCop were found to be low; however, the alloy tested is noted as GlidCop Al-10, which contains 0.2 wt.% Al₂O₃^[4] versus 0.32 wt.% Al₂O₃ for GlidCop Al-15.

Cu-0.9Cr is precipitation strengthened by elemental Cr precipitates and is known for excellent cold workability. Precipitation hardening for these alloys consists of solution treatments near 990 °C for about 20 minutes, water quenching, and aging near 460 °C for about 3 hours.^[12] Near peak strength in Cu-0.9Cr alloys is sometimes achieved during processing, due either to cold work, or precipitation hardening at process temperatures. In such cases only moderate gains in strength are possible with aging heat treatments.^[13] The ductility of these alloys near the expected use temperatures of 400 to 600 °C has been found to be poor compared to other copper alloys.^[5,6] Room temperature strength in Cu-0.9Cr alloys is good, with UTS values near 500 MPa.^[4,5,6] Strength declines with increasing temperature, particularly steeply as 427 °C is exceeded, with UTS values near 65 MPa at 593 °C.^[5,6]

Cu-1Cr-0.1Zr is age hardenable, with Cr and Cu₅Zr precipitates.^[16] Pratt & Whitney presented work on an alloy, Cu-1Cr-0.5Zr, which was found it to be very strong, but to have poor low cycle fatigue at 705 °C compared to NARloy-Z and a Cu-0.47wt% Zr alloy (which is close to the composition of AMZIRC).^[17] The literature data indicates that at 538 °C, on the basis of total axial strain range versus number of cycles to failure, the fatigue properties of AMZIRC, and Cu-Zr alloys are better than those of Cu-Cr, NARloy-Z, and GlidCop Al-10.^[4,5,7] Ultimate and yield strengths at 705 °C for as-received material were approximately 175 and 94 MPa respectively. Tensile properties for Cu-Cr-Zr alloys are also reported by Zinkle.^[18] The solution and aging temperatures for Cu-1Cr-0.1Zr are expected to be similar to AMZIRC and Cu-0.9Cr. The solution and aging temperatures for Cu-0.9Cr are approximately 990 and 440 °C respectively. The effectiveness of aging also depends on quench rates from solution temperatures. Relations between quench rates and hardenability in the Cu-1Cr-0.1Zr alloy were also examined as part of this work but are reported elsewhere.

Although no new tests were done with the alloy known as NARloy-Z, for completeness, data was drawn from the literature and included in some figures and comparisons to the other alloys. NARloy-Z is a Cu-3Ag-0.5Zr alloy that is currently used in NASA's Space Shuttle Main Engines. A chemically equivalent alloy known as NASA-Z has been used by Aerojet as a liner material in several of Aerojet's rocket combustion chambers.^[14] These copper-silver-zirconium alloys are typically solution treated, water quenched, and aged for maximum strength, forming zirconium and silver rich precipitates. Nguyentat, Gibson and Horn have examined relations among quench rates from the solution temperature.^[14] Hardness and yield strength declined by a factor of 3 when water quench rates from the solution temperature were decreased to those achieved through furnace cooling, however ultimate tensile strength declined only about 13%. Room temperature maximum ultimate tensile strengths for NARloy-Z and NASA-Z are typically 320 MPa, with yield strengths around 170 MPa,^[3,9,14,15,19] these have been shown to decline as a result of exposure to high temperatures, such as due to a brazing heat treatment. The yield strength of NARloy-Z after a brazing heat treatment has been found to be approximately 80 MPa at 100 °C.^[3]

Test Procedures

The test plan included tensile, compressive, creep, thermal expansion and low-cycle fatigue properties of all the alloys. Low-cycle fatigue results will be presented elsewhere. Detailed testing procedures have been presented previously^[20-23] and will be only briefly outlined here.

All alloys were tested in both the as-received condition and after a simulated braze treatment. GRCop-84 was tested in two as-received conditions: as-extruded, and as-HIPed. AMZIRC, GlidCop Al-15, Cu-1Cr-0.1Zr, and Cu-0.9Cr alloys were received in the form of hard drawn rods that were 3/8 to 3/4 inch diameter. Table 2 shows the simulated braze cycle designated “Braze 935” which is meant to be typical of a main combustion chamber liner/jacket brazing operation.

Tensile and Creep Procedures

Tensile and compression tests were conducted at 25, 200, 500, 650, and 800 °C (77, 392, 932, 1202, and 1472 °F) using strain rate control. Tests at elevated temperatures employed flowing Ar at 2.5 l/min. A strain rate of 0.005 mm/mm/min ($8.3 \times 10^{-5} \text{ sec}^{-1}$) was used in both tensile and compression tests. Strain was measured via an extensometer attached to the gage of the tensile samples, but compression tests relied on crosshead displacement. Specimen dogbones used for AMZIRC, Cu-1Cr-0.1Zn, and Cu-0.9Cr tensile and creep tests had a gauge diameter and length of 5.84 mm (0.23 in) and 29.06 mm (1.144 in) respectively. Tensile and creep GlidCop Al-15 specimens used a gauge diameter and length of 9.02 mm (0.355 in) and 40.82 mm (1.607 in) respectively. Compression specimens were cylinders of 5.0 mm (0.197 in) diameter by 10 mm (0.394 in) long.

Creep tests were done in vacuum at 500, 650, and 800 °C using constant load lever arm vacuum creep units. The stresses in the creep tests were varied to give lives equivalent to 100 Space Shuttle missions (15 hours). For GRCop-84 creep stresses were about 100 MPa at 500 °C, 40 MPa at 650 °C, and 20 MPa at 800 °C. Stress levels for the other alloys typically had to be lower to achieve lives near 15 hours.

Creep testing of all alloys except GRCop-84 started with step loading vacuum creep tests using a converted Instron tensile test load frame. The load was held constant for five hours, and then raised a set amount every five hours for a total of 20 steps, or until failure. All creep tests were performed with at least two thermocouples attached to the ends of the gage area. For these creep tests, strain was measured by monitoring crosshead movement. All creep rates were defined as the slope of the linear portion of the creep strain-time curve between primary and tertiary creep.

In an effort to include previous constant load GRCop-84 creep tests, we have statistically modified some older GRCop-84 data to make it consistent with the methods used in this study. These data were then used to determine power law creep coefficients for comparison to the other alloys (see Table 4). The details of the statistical processing are in Ref. 24. These creep rate equations for GRCop-84 were plotted with the constant load creep data in Fig. 16.

Thermal Expansion Procedures

Thermal expansion of the candidate alloys was conducted using an Anter Unitherm 1161AL-V vertical two head pushrod dilatometer. Resolution of the displacement was 0.001 mm. A sample was loaded along with a Pt standard, and the chamber sealed. The chamber was evacuated and purged with argon several times to remove the oxygen from the chamber. During the final purge the pressure was reduced to $\leq 39 \text{ Pa}$ (300 millitorr) prior to backfilling with Ar. Ar was selected over He based upon the tendency of Ar to collect at the bottom of the chamber and displace any residual oxygen in the vicinity of the sample.

The samples were heated to 1000 °C using a heating rate of 3 °C per minute and then cooled to room temperature while the changes in length for both the copper alloy sample and Pt standard were measured. During cooling the rate was 3 °C per minute until the temperature reached approximately 175 °C. At that point the samples underwent free cooling. Ar was flowing through the chamber during the test at a rate of approximately 50 cm³ per minute. This maintained the chamber at a slight positive pressure. Oxidation of the samples was minimal and did not affect the results. Each sample was given five cycles. Two samples of each alloy were tested.

During the test the displacement and temperature for both samples were measured simultaneously. Using the sample temperature and reference data for the thermal expansion of Pt,^[25] the actual displacement from the Pt sample's thermal expansion could be calculated for each data point. Subtracting this value from the measured displacement of the Pt sample allowed the calculation of the contribution of the thermal expansion of the alumina push rod and sample holder to the observed displacements. The contribution of the holder and push rod was then subtracted from the measured copper alloy displacement to calculate the actual thermal expansion of the Cu alloy sample at each data point. To calculate the thermal expansion strain, the displacement was divided by the original sample length. The data was then plotted and fitted with a second order polynomial equation. The thermal expansion of each specimen was measured five times, the results of these five cycles were averaged, and then the results of two specimens were averaged to yield the final empirical relations between thermal expansion and temperature.

Test Results

Microstructures

Figure 1 shows typical as-extruded GRCop-84 microstructure. The as-HIPed and brazed microstructures are visually indistinguishable from the as-extruded microstructure. GRCop-84 gains most of its added strength over pure copper from finely dispersed Cr_2Nb precipitates such as those shown in Fig. 1. The stability and melting point of Cr_2Nb is so high that it begins to precipitate in the molten GRCop-84 before the onset of primary Cu solidification.^[26] These stable Cr_2Nb precipitates do not significantly coarsen during the brazing heat treatment or during use at high temperatures.

Figures 2 and 3 show the as-received and post brazed microstructures for AMZIRC. In Fig. 3 it can be seen that the fine, elongated grain structure observed in as-received hard drawn AMZIRC (Fig. 2) has given way to a much coarser structure of equiaxed grains with some twinning indicative of complete recrystallisation and considerable grain growth. The observed twinning is common for FCC metals during recrystallization.^[27] Rather large ($\sim 5 \mu\text{m}$) precipitates are present in both as-received and brazed structures. These precipitates are believed to be high temperature Cu_5Zr intermetallics formed during casting and not solutionized at the brazing temperature or at the solution temperatures normally used for AMZIRC (980 °C).

The recrystallized grains in the brazed AMZIRC are essentially strain free. This lower dislocation density contributes to the decline in strength upon brazing as does the larger grain size through a Hall-Petch relationship.^[27]

Figures 4 and 5 show the as-received and post brazed microstructures of GlidCop Al-15. As was the case for GRCop-84, the microstructure of GlidCop appears to be unaffected by the simulated braze heat treatment.

Figures 6 and 7 show the microstructures of as-received and post brazed Cu-1Cr-0.1Zr. The as-received Cu-1Cr-0.1Zr has a fine grain structure, elongated along the drawing direction. The brazed material has recrystallized; but the grain size appears to have remained small, maybe even decreased compared to the as-received Cu-1Cr-0.1 material. Thus the presence of Cr in the alloy prevented the extensive grain growth observed in AMZIRC after recrystallisation. What we believe to be Cr and Cu_5Zr precipitates can be seen in the high magnification micrographs (Figs. 6(b), and 7(b)). The Cu_5Zr precipitates, which have a melting point near 1030 °C, have an alignment due to the drawing process; since this alignment persists in the brazed microstructure it is concluded that the Cu_5Zr precipitates are not solutionized at the 935 °C brazing temperature, which is consistent with the ternary Cu-Cr-Zr phase diagram of Zeng et al.^[16]

The Cu-0.9Cr structures shown in Figs. 8 and 9 appear nearly identical to those seen in Cu-1Cr-0.1Zr, with the structure of the Cu-0.9Cr alloy consisting of fine, slightly elongated grains and Cr precipitates in the as-received microstructures. The braze appears to have caused recrystallization (Fig. 9) but extensive grain growth did not occur, as it did in the case of AMZIRC. The aligned precipitates in the as-received structure (Fig. 8(b)) appear much more spherical after brazing (Fig. 9(b)).

Tensile and Compression Tests

Room and elevated temperature tensile and compressive properties for the alloys are presented in Figs. 10 through 18. In Figs. 10 through 13, data points shown for GRCop-84 are from an average of five tests. Data points for AMZIRC are from the average of two tests except at the temperatures of 400, 500, 600, and 650 °C which were single tests. The data points for GlidCop Al-15, Cu-1Cr-0.1Zr, and Cu-0.9Cr were from the average of two tests. The compression data shown in Fig. 14 were averaged from two or three tests. Tables containing these data are presented in Ref. 20.

The ultimate and yield strengths shown in Figs. 10 and 11 indicate that in the as-received condition the competing alloys, AMZIRC, GlidCop, Cu-1Cr-0.1Zr, and Cu-0.9Cr are generally stronger than GRCop-84. However, after the simulated brazing heat treatment, the strength of AMZIRC, Cu-1Cr-0.1Zr and Cu-0.9Cr drop dramatically to strength levels significantly below GRCop-84. GlidCop Al-15 retains most of its strength after the brazing heat treatment making it stronger than GRCop-84 in tensile tests at all temperatures and conditions examined. NARloy-Z's ultimate strength is similar to GRCop-84's, however NARloy-Z's yield strength is lower, particularly after brazing. There is an abrupt drop in the strength of as-received AMZIRC near 500 °C which appears to coincide with the onset of annealing and recrystallization. The strength of Cu-1Cr-0.1Zr and Cu-0.9Cr drop more gradually as test temperatures are increased compared to AMZIRC. The trends apparent in the tensile strengths of the alloys are mirrored in compression as shown in Fig. 14.

All failures were ductile except those for Cu-0.9Cr at temperatures between 500 and 650 °C. At these temperatures the ductility of Cu-0.9Cr was the lowest of all the alloys, with elongation and reduction in area being approximately 2 and 6.7% respectively. Exposing as-received AMZIRC to temperatures above 500 °C

approximately tripled elongation, resulting in the highest elongations of any of the alloys (Fig. 12). GRCop-84 and GlidCop Al-15 had approximately the same elongation. In general, it was found that as the testing temperature increased, uniform elongation increased and localized necking decreased which decreased the reduction in area measurements (R/A) as shown in Fig. 13. At temperatures above 500 °C reduction in area was higher for GRCop-84 compared to GlidCop Al-15.

Creep Tests

Results of step loading creep tests are shown in Fig. 15. Constant load creep results are shown in Fig. 16. All creep rates, or strain rates measured during creep tests, were defined as the linear portion of the time – strain data after load up and primary creep but before tertiary creep.

It can be seen in Fig. 15 that at a given stress at 500 °C the steady-state creep rate of as-received AMZIRC is about double that of GRCop-84, and the strain rate of brazed AMZIRC is about two orders of magnitude greater than GRCop-84. Similarly, strain rates of AMZIRC at 650 °C at a stress of 20 MPa are about two orders of magnitude greater than the strain rates observed for GRCop-84 at 650 °C and 20 MPa. NARloy-Z and Cu-0.9Cr also performed much worse than GRCop-84 in creep. In the as-received condition GlidCop-Al15 and Cu-1Cr-0.1Zr performed better than GRCop-84, however, Cu-1Cr-0.1Zr's creep properties suffered after brazing.

From our experience, a creep rate of about $5 \times 10^{-6} \text{ sec}^{-1}$ often yields a creep rupture life of about 15 hours assuming most of the creep life is spent in second stage or steady-state creep. Step loaded and constant load creep tests indicate that at 500 °C stresses of about 65 and 130 MPa applied to brazed AMZIRC and GRCop-84 respectively are expected to yield approximately, 15 hour lives (Figs. 15 and 16). Thus for equivalent temperatures and lives, GRCop-84 can sustain about double the creep stress compared to brazed AMZIRC. Note how close together the GRCop-84 (650 °C) and brazed AMZIRC (500 °C) curves are in Fig. 15. This indicates that at equivalent stress and strain rate, such as $\sigma = 47 \text{ MPa}$ and $\dot{\epsilon} = 10^{-6} \text{ sec}^{-1}$, GRCop-84 can operate at temperatures 150 °C higher than AMZIRC. GlidCop Al-15 performed very well, with creep rates much lower (at a given stress) than any of the other alloys at 500 °C. As-received Cu-1Cr-0.1Zr also performed very well in creep, however, after brazing, creep properties declined substantially such that GRCop-84 was found to withstand double the stress at equivalent strain rates at 650 °C.

Often creep can be described by a rate equation of the form $\dot{\epsilon} = A\sigma^n$, where $\dot{\epsilon}$ is creep strain rate, A is a constant, σ is creep stress, and n is the stress exponent. The power law creep constants for the step loaded creep tests and those resulting from the constant load creep tests were independently determined and are presented in Tables 3 and 4. The stress exponent n can help to identify creep mechanisms,^[28] for example, dispersion strengthened materials commonly have high stress exponents, of the order of 20 to 100 due to the added resistance to dislocation glide caused by the particles. Before such an exploration of creep mechanisms, trends in our data, and areas where more data are needed will be examined. The creep stress exponents n for GRCop-84 at 500, 650 and 800 °C were fairly consistent, equal to about 9.5 in the step loaded creep tests, and 8 for constant load creep.^[24] The stress exponents for GlidCop ranged from 12.4 to 91.2 (see Tables 3 and 4) and the exponents resulting from step loaded creep (Table 3) were consistently and significantly lower than the exponents resulting from constant load creep (Table 4). The stress exponents for AMZIRC averaged about 5.3 (with a range of 2.35 to 9.49), n averaged about 5.1 for the Cu-1Cr-0.1Zr creep tests, and the average stress exponent for the Cu-0.9Cr tests was 4.4.

Thermal Expansion

Thermal expansion results are presented in Fig. 17 and Table 5. Figure 17 shows plots of the equations presented in Table 5. The best fit equation for GRCop-84 with two-way confidence intervals taken from Ref. 29 is:

$$\alpha(T) = \left(-0.3287 + 2.265 \times 10^{-4} T^{1.285} \right) \pm t \left(1 - \frac{\alpha}{2}, 10 \right) \sqrt{ \left(1.403 \times 10^{-2} \right)^2 + \left(2.038 \times 10^{-5} T \right)^2 } \quad (1)$$

where T is in Kelvin, $t(1-\alpha/2, 10)$ is the value for the t -distribution with 10 degrees of freedom associated with $1-\alpha/2$ cumulative probability, and $\alpha(T)$ is the thermal expansion of GRCop-84 in percent ($\alpha(T)/100\%$ is plotted in Fig. 17). The four alloys being compared to GRCop-84 have about the same thermal expansion. This is expected since they are all near 99% Cu. GRCop-84 however has about 14 vol.% Cr₂Nb which retards temperature driven strains, and results in thermal expansion being between 7 and 15% lower for GRCop-84 than the other alloys at typical liner hot wall temperatures.

Discussion

Comparison of Properties

Desirable properties for copper alloys being developed for rocket engine components include: low thermal expansion; high strength; high ductility; ease of processing; low creep rate; high compressive strength; high low-cycle-fatigue strength; high maximum operating temperature; and a minimum affect caused by component manufacture such as brazing. The data presented in this paper and the literature were considered in the comparison of GRCo-84 to the other alloys. A summary of this comparison is presented in Table 6.

High temperature creep in alloys involves the interaction of the stress fields of moving dislocations with those of stationary dislocations and other boundaries such as second phase particles and grain boundaries. Specific values of the stress exponent n are associated with particular creep mechanisms. Alloys that exhibit pure metal (or “class M”) behavior are characterized by $n = 4$ to 8; exponent values in this range can be taken as evidence that the creep mechanism is dominated by dislocation climb. A majority of the creep data indicates that AMZIRC, Cu-0.9Cr, and Cu-1Cr-0.1Zr have stress exponents in this range, indicating dislocation climb, or class M, creep.

Due to added interactions between dislocations and fine particles, dispersion strengthened materials usually have stress exponents of the order of 10 to 100. This enhanced sensitivity to stress is believed to be due to the added energy required for dislocations to climb out of their glide planes to overcome the particles and the thermally activated release of those dislocations from the departure side of the particles.^[28] GlidCop Al-15 had n values between 12 and 91, which are considered to be characteristic of dispersion strengthened alloys. Though data was limited, GRCo-84 had stress exponents in the range of 7.3 to 10, implying class M creep behavior (dislocation climb) with some added stress sensitivity resulting from the relatively large volume fraction of precipitates and grain boundaries.

Refer to Table 6 for comparisons of thermal conductivity and expansion, tensile and compressive strength, ductility, creep, and the effects of brazing on the alloys.

Microstructure-Property Relations

Microstructures are shown in Figs. 1 through 9. The large number of Cr₂Nb precipitates present in GRCo-84 (Fig. 1) result in good strength, and since the precipitates are stable and do not significantly coarsen, properties decline moderately with increasing temperature. The same can be said for GlidCop Al-15 (Figs. 4 and 5) microstructurally, though the precipitate is alumina. The microstructural feature that dominates properties in GRCo-84 and GlidCop is the stable precipitates. These precipitates enabled GRCo-84 and GlidCop to perform significantly better than the precipitation strengthened alloys in the brazed condition in both strength and creep.

By contrast, the microstructure of AMZIRC is dominated by the fine elongated grain boundaries and the benefits of work hardening (Figs. 2 and 3). Though the as-received microstructures of Cu-1Cr-0.1Zr and Cu-0.9Cr had some grain texturing characteristic of longitudinally drawn material, this elongation of fine grains was by far the most pronounced in AMZIRC; these fine textured grains, combined with precipitation hardening, result in excellent as-received strengths at temperatures below 500 °C in AMZIRC. Precipitates in as-received AMZIRC appear coarser than those present in Cu-1Cr-0.1Zr which likely contributes to the higher strength in Cu-1Cr-0.1Zr. Figure 3 shows this fine grain structure in AMZIRC is destroyed at brazing temperatures, and Fig. 10 shows the resulting drop in strength.

The microstructures of as-received and brazed Cu-1Cr-0.1Zr and Cu-0.9Cr look nearly identical. Recrystallisation appears to have occurred in AMZIRC, Cu-1Cr-0.1Zr, and Cu-0.9Cr during brazing, but, subsequent grain growth and coarsening occurred in AMZIRC only. Chromium appears to have prevented significant grain growth during brazing in the Cu-1Cr-0.1Zr and Cu-0.9Cr alloys. The finer post braze microstructures in Cu-1Cr-0.1Zr and Cu-0.9Cr appear to help little in terms of improved properties. The coarser brazed AMZIRC has about the same strength and creep properties as Cu-1Cr-0.1Zr and Cu-0.9Cr. The differences that stand out among *brazed* Cu-1Cr-0.1Zr, Cu-0.9Cr, and AMZIRC are: AMZIRC has the lowest yield strength (though ultimate strengths are similar); Cu-0.9Cr has significantly poorer creep properties; and as-received Cu-0.9Cr had markedly inferior ductility.

Property Implications on Alloy Selection

The heat treatable alloys (AMZIRC, Cu-1Cr-0.1Zr, and Cu-0.9Cr) have excellent as-received properties. The exceptions observed in this work were that Cu-0.9Cr and NARloy-Z have relatively poor creep properties in the as-received and brazed conditions compared to all the other alloys. NARloy-Z had the lowest as-received yield strength

and was weakened substantially after brazing. Thus if use temperatures are below 500 °C, and no high temperature (>500 °C) processing is required for the alloy, AMZIRC and Cu-1Cr-0.1Zr are advantageous.

The high temperature stability of GlidCop Al-15 and GRCop-84 resulted in superior properties compared to the other alloys in the brazed condition. Ultimate and yield strengths, compressive yield strength, and creep stress at a given strain rate were all about two to three times greater in GlidCop and GRCop-84 compared to the other alloys after the simulated braze heat treatment. Thus if use or processing temperatures in excess of 500 °C are expected, GlidCop Al-15 and GRCop-84 have solid advantages in strength and creep over AMZIRC, Cu-1Cr-0.1Zr, Cu-0.9Cr, and NARloy-Z.

It may be possible to regain some of the strength lost during the brazing operation in the heat treatable alloys if the alloy is quenched rapidly enough from the brazing temperature (which is also acting as the solution temperature). This might nullify the post braze advantages noted for GlidCop and GRCop-84, but only for use temperatures below 500 °C, or for short term use near 500 °C. This issue is discussed in more detail elsewhere.^[20]

Summary and Conclusions

In the as-received condition at <500 °C, AMZIRC, GlidCop Al-15, Cu-1Cr-0.1Zr, and Cu-0.9Cr were all stronger in tension and compression than GRCop-84. However, after a simulated braze heat treatment at 935 °C, the strengths of the precipitation strengthened AMZIRC, Cu-1Cr-0.1Zr, Cu-0.9Cr and NARloy-Z drop to levels significantly below the strength of GRCop-84 at all temperatures. The strength of dispersion strengthened GlidCop Al-15 was largely unaffected by the heat treatment at 935 °C, thus GlidCop retained strength levels above those of GRCop-84 at all temperatures.

Ductility was lowest in as-received Cu-0.9Cr. Ductility was also low for GlidCop Al-15 and in HIPed GRCop-84. The reduction in area was particularly low in GlidCop Al-15 above 500 °C. Cu-1Cr-0.1Zr and AMZIRC had much greater reductions in area and elongations than the other alloys.

Creep properties were best for as-received Cu-1Cr-0.1Zr and GlidCop Al-15 and worst for Cu-0.9Cr and NARloy-Z. After the simulated braze at 935 °C GRCop-84 and GlidCop had markedly better creep properties compared to the other alloys. At equivalent stress and strain rates, GRCop-84 showed a 150 °C advantage over AMZIRC in the brazed condition. Alternatively, at equivalent temperature and strain rates, GRCop-84 was twice as strong as brazed AMZIRC. Our tests indicate GlidCop Al-15 to be more resistant to creep at 500 °C than GRCop-84, with creep rates two orders of magnitude lower than GRCop-84's at equivalent stress. This work has found that:

- After brazing, GRCop-84 and GlidCop Al-15 are stronger than AMZIRC, Cu-1Cr-0.1Zr, Cu-0.9Cr, and NARloy-Z;
- After brazing, GRCop-84 and GlidCop Al-15 are superior to AMZIRC, Cu-1Cr-0.1Zr, Cu-0.9Cr, and NARloy-Z in high temperature creep;
- Due to better ductility and processing characteristics GRCop-84 has advantages over GlidCop Al-15;
- The heat treatment used might be a worst case example for the heat treatable alloys (AMZIRC, Cu-1Cr-0.1Zr, and Cu-0.9Cr). Although strength gained from cold work will be lost at brazing temperatures, it might be possible to recuperate some strength by combining solutionizing, quenching and aging cycles with the brazing operation.

Acknowledgements

We would like to praise and acknowledge the dedicated support of our technicians and machine shop personnel: John Zoha, Sharon Thomas, Bill Armstrong, John Juhas, Adrienne Veverka, Ronald Phillips, Dave Brinkman, Aldo Panzanella, and Tim Ubienski; as well as our furnace/heat treat engineer Mark Jaster. Their support has enabled timely progress on this effort.

References

1. D.T. Butler Jr. and M.J. Pindera, "Analysis of Factors Affecting the Performance of RLV Thrust Cell Liners," NASA/CR—2004-213141, Aug. 2004.
2. J.J. Stephens and D.T. Schmale, "The effect of high temperature braze thermal cycles on mechanical properties of a dispersion strengthened copper alloy," SAND87-1296 • UC-20, 1987, 1988 second printing.
3. M.V. Nathal, D.L. Ellis, W.S. Loewenthal, S.V. Raj, L.U. Thomas-Ogbuji, J. Ghosn, L.A. Greenbauer-Seng, J. Gayda, and C.A. Barrett, "High conductivity materials for high heat flux applications in space propulsion systems," JANNAF 39th CS/27th APS/21st PSHS/3rd MSS Subcommittee Joint Meeting, Colorado Springs, CO, CD-ROM, (Dec. 2003), p. 2003-0390cc.

4. J.B. Conway, R.H. Stentz, and J.T. Berling, "High temperature, low cycle fatigue of copper-base alloys in argon; Part I—Preliminary results for 12 alloys at 1000 °F (538 °C)," NASA CR–121259, 1973.
5. P.A. Wycliffe, "Literature search on high conductivity copper based alloys," Final Report IDWA No. 6458–2, Rockwell International Sci. Center, R5739TC/sn, 1984.
6. D.D. Horn and H.F. Lewis, "Property Investigation of Copper Base Alloys at Ambient and Elevated Temperatures," AEDC–TR–65–72, 1965, (Defense Document Center No. 467015) p. 4, 11, 12, 35, 38.
7. J.B. Conway, R.H. Stentz, and J.T. Berling, "High-Temperature, Low-Cycle Fatigue of Copper-Base Alloys for Rocket Nozzles, Part II—Strainrange Partitioning and Low-Cycle Fatigue Results at 538 °C," NASA CR–135073, 1976.
8. N.P. Hannum, H.J. Kasper, and A.J. Pavli, "Experimental and Theoretical Investigation of Fatigue Life in Reusable Rocket Thrust Chambers," AIAA/SAE 12th Propulsion Conf., AIAA Paper No. 76–685, 1976.
9. J.J. Esposito and R.F. Zabora, "Thrust Chamber Life Prediction—Vol. I—Mechanical and Physical Properties of High Performance Rocket Nozzle Materials," NASA CR–134806, 1975.
10. E.N.C. Dalder, W. Ludemann, and B. Schumacher, "Thermal stability of four high-strength, high-conductivity copper sheet alloys," UCRL–88919, and ASM's Copper and Copper Alloys Conf., 1983, material also appears in UCRL–89034–Rev. 1, Conf-830466-Rev-1, DE83 013312 Accession No. 84N10288, DOE Workshop on Copper Alloys, 1983.
11. J.J. Stephens, R.J. Bourcier, F.J. Vigil, and D.T. Schmale, "Mechanical properties of dispersion strengthened copper: a comparison of braze cycle annealed and coarse grain microstructure," Sandia Report SAND88–1351, 1988.
12. *Metals Handbook*, 9th ed., Properties and Selection: Nonferrous Alloys and Pure Metals, ASM Handbook Committee, American Soc. for Metals, Metals Park, OH, 1979, **2**, p. 309.
13. J.B. Correia, H.A. Davies, and C.M. Sellars, "Strengthening in rapidly solidified age hardened Cu-Cr and Cu-Cr-Zr alloys," *Acta mater.*, **45**, (1), 1997, pp. 177–190.
14. T. Nguyentat, V.A. Gibson, and R.M. Horn, "NASA-Z A liner material for rocket combustion chambers," 27th Joint Prop. Conf., AIAA Paper No. 91–2487.
15. D.L. Ellis, "GRCop-84: A high-temperature copper alloy for high-heat-flux application," NASA/TM—2005-213566.
16. K.J. Zeng, M. Hamalainen, and K. Lilius, "Phase relationships in Cu-rich corner of the Cu-Cr-Zr phase diagram," *Scripta Metallurgica et Materialia*, **32**, (12), 1995, pp. 2009–2014.
17. Pratt & Whitney Aircraft Group: "Thrust Chamber Material Technology Program," NASA CR–187207, 1989.
18. S.J. Zinkle, "Tensile properties of high-strength, high-conductivity copper alloys at high temperatures," in *Fusion Materials Semiann. Prog. Report for period ending June 30, 2000*, DOE/ER–0313/28, Oak Ridge National Lab, Oak Ridge, TN, 2000, pp. 171–175.
19. J.M. Kazaroff and G.A. Repas, "Conventionally Cast and Forged Copper Alloy for High Heat Flux Thrust Chambers," NASA Technical Paper 2694, NASA Glenn Research Center, Cleveland OH, 1987.
20. H.C. de Groh III, D.L. Ellis, and W.S. Loewenthal, "Comparison of GRCop-84 to other High Thermal Conductive Cu Alloys," NASA/TM—2007-214663, NASA Glenn Research Center, Cleveland, OH, 2007.
21. D.L. Ellis and R.L. Dreshfield, "Preliminary evaluation of a powder metal copper-8 Cr-4 Nb alloy," in *Advanced Earth-to-Orbit Propulsion Technology 1992*, NASA CP–3174, **1**, NASA Marshall Space Flight Center, Huntsville, AL, May 1992, pp. 18–27.
22. D.L. Ellis, R.L. Dreshfield, M.J. Verrilli, and D.G. Ulmer, "Mechanical Properties of a Cu-8 Cr-4 Nb alloy," in *Advanced Earth-to-Orbit Propulsion Technology 1994*, NASA CP–3282, NASA Marshall Space Flight Center, Huntsville, AL, May 1994, pp. 32–41.
23. D.L. Ellis and G.M. Michal, "Mechanical and thermal properties of two Cr-Cr-Nb alloys and NARloy-Z" NASA CR–198529, NASA Glenn Research Center, Cleveland OH, Oct. 1996.
24. D.L. Ellis, W.S. Loewenthal, and H. Haller, "Creep of Commercially Produced GRCop-84," NASA TM to be published, NASA Glenn Research Center, Cleveland, OH, 2007.
25. A. Goldsmith, T.E. Waterman, and H.J. Hirschhorn, *Handbook of Thermophysical Properties of Solid Materials*, **1**, Pergamon, New York, NY, 1961.
26. D.L. Ellis and G.M. Michal, "Formation of Cr and Cr₂Nb precipitates in rapidly solidified Cu-Cr-Nb ribbon," *Ultramicroscopy*, **30**, (1–2), June 1989, pp. 210–216.
27. J.D. Verhoeven, *Fundamentals of Physical Metallurgy*, John Wiley & Sons pub., 1975, p. 330, 459, 515–517.
28. *ASM Handbook*, **8**, Mechanical Testing and Evaluation, H. Kuhn and D. Medlin, eds., ASM International, 2000, pp. 363–368.
29. D.L. Ellis and D.J. Keller, "Thermophysical Properties of GRCop-84," NASA/CR—2000-210055, NASA Glenn Research Center, Cleveland, OH, June 2000.

Table 1 Composition of Cu alloys in weight percent.

Alloy	Cr	Nb	Zr	Al	O	Ag
GRCop-84	6.65	5.85				
AMZIRC (C15000)			0.15			
GlidCop Al-15 (C15715)				0.15	0.17	
Cu-0.9Cr (C18200)	0.9					
Cu-1Cr-0.1Zr (C18150)	1.0		0.1			
NARloy-Z			0.5			3.0

Table 2 Simulated braze heat treatment.

Stage	Action
1	Raise temperature from 25 to 935 °C
2	Hold at 935 °C for 22.5 ± 2.5 min
3	Lower temperature from 935 to 871 °C at 1.7 °C/min
4	Lower temperature from 871 to 538 °C at 2.8 °C/min
5	Free cool to room temperature and remove specimen from furnace

Table 3 Power function constants for step loaded, secondary steady state creep; creep rate power functions of the form $\dot{\epsilon} = A\sigma^n$ where A and n are given in the table, $\dot{\epsilon}$ is creep rate in units of sec^{-1} , and σ is step loaded creep stress in units of MPa.

	A	n
GRCop-84 as-received, 500 °C	4.77E-26	9.49
GRCop-84 as-received, 650 °C	7.17E-24	10.32
GRCop-84 as-received, 800 °C	2.63E-18	8.67
AMZIRC as-received, 500 °C	4.15E-20	6.70
AMZIRC Brazed, 500 °C	4.18E-13	3.73
AMZIRC as-received, 650 °C	*	*
AMZIRC Brazed, 650 °C	2.99E-11	3.65
GlidCop as-received, 500 °C	7.71E-57	22.93
GlidCop Brazed, 500 °C	3.72E-34	12.40
GlidCop as-received, 650 °C	4.58E-39	15.90
GlidCop Brazed, 650 °C	8.48E-38	15.50
Cu-1Cr-0.1Zr as-received, 500 °C	1.47E-19	5.59
Cu-1Cr-0.1Zr Brazed 500 °C	5.94E-17	5.71
Cu-1Cr-0.1Zr as-received 650 °C	1.01E-13	5.03
Cu-1Cr-0.1Zr Brazed 650 °C	1.50E-14	5.52
Cu-0.9Cr as-received 500 °C	7.31E-18	6.04
Cu-0.9Cr Brazed, 500 °C	4.00E-14	5.08
Cu-0.9Cr as-received 650 °C	*	*
Cu-0.9Cr Brazed 650 °C	1.27E-10	3.83

*Insufficient data to obtain constant

Table 4 Power function constants for constant load, secondary, steady state tensile creep at elevated temperatures; creep rate power functions of the form $\dot{\epsilon} = A\sigma^n$ where A and n are given in the table, $\dot{\epsilon}$ is creep rate in units of sec^{-1} , and σ is constant load creep stress in units of MPa.

	A	n
GRCop-84, 500 °C	1.042E-22	7.67
GRCop-84 650 °C	3.400E-21	8.52
GRCop84 800 °C	1.078E-16	7.3
Amzirc as-received, 500 °C	8.919E-13	2.35237
Amzirc Brazed, 500 °C	1.633E-23	9.48610
Amzirc as-received, 650 °C	2.638E-10	3.55738
Amzirc Brazed, 650 °C	2.141E-17	7.80399
GlidCop as-received, 500 °C	2.392E-87	36.40497
GlidCop Brazed, 500 °C	1.195E-205	91.21151
GlidCop as-received, 650 °C	3.312E-61	26.74301
GlidCop Brazed, 650 °C	2.762E-56	24.69575
CuCrZr as-received, 500 °C	6.857E-20	5.46637
CuCrZr Brazed 500 °C	2.489E-14	4.46268
CuCrZr as-received 650 °C	4.040E-10	2.13871
CuCrZr Brazed 650 °C	8.059E-17	7.07106
CuCr as-received 500 °C	6.353E-13	3.01887
CuCr Brazed, 500 °C	7.363E-13	4.17238
CuCr as-received 650 °C	*	*
CuCr Brazed 650 °C	6.047E-11	4.05855

*Did not follow power law creep.

Table 5 Thermal expansion of AMZIRC, GlidCop Al-15, Cu-1Cr-0.1Zr, and Cu-0.9Cr alloys where the thermal expansion, α , in units of in/in, is expressed as a quadratic function of temperature, T , in units of °C, such that $\alpha(T) = A(T)^2 + B(T) + C$. Based on the variations of α expressed among different specimens, α values are estimated to be accurate to within $\pm 1\%$.

Alloy	A	B	C
AMZIRC	4.132E-09	1.610E-05	-1.701E-04
GlidCop Al-15	3.989E-09	1.619E-05	-1.000E-04
Cu-1Cr-0.1Zr	4.947E-09	1.559E-05	-8.019E-05
Cu-0.9Cr	4.317E-09	1.599E-05	-1.016E-04

Table 6 Summary and comparison of alloy properties.

Property	Comparison
Thermal conductivity	The conductivity of oxygen free copper is about 400 W/mK, all alloys of copper are below this value. The conductivity of AMZIRC is best at about 370 W/mK, the conductivity of GlidCop Al-15 and NARloy-Z is approximately 320 W/mK, and that of GRCop-84 is about 300 W/mK. ^[3]
Thermal expansion	The thermal expansion of GRCop-84 is the lowest at 0.008 in/in at 480 °C; the expansion of GlidCop, AMZIRC, Cu-1Cr-0.1Zr, and Cu-0.9Cr at this temperature are all about the same at 0.0087 in/in.
Strength	Since GlidCop and GRCop-84 are not significantly influenced by high temperature brazing, these two alloys are clearly stronger than the heat treatable alloys (AMZIRC, Cu-1Cr-0.1Zr, Cu-0.9Cr, NARloy-Z) after brazing. In the absence of any brazing heat treatment – Cu-1Cr-0.1Zr is strongest, even at test temperatures up to 650 °C. However, the strength of Cu-1Cr-0.1Zr is expected to degrade with time at use temperatures in excess of 500 °C due to over aging.
Compressive strength	Compressive strength in these alloys closely follows what was found for tensile strength. GlidCop Al-15 and GRCop-84 were the strongest after brazing.
Ductility	GRCop-84, AMZIRC, and Cu-1Cr-0.1Zr all had good ductility. GRCop-84's elongation was the most consistent, remaining between about 16 and 25% across the entire temperature range tested (20 to 800 °C). GlidCop Al-15 and Cu-0.9Cr had the worst ductility at temperatures greater than 500 °C; the ductility of Cu-0.9Cr was particularly bad (~2% elongation) at 500 and 650 °C.
Creep	GlidCop Al-15 had the best creep properties of all the alloys regardless of brazing condition. The creep properties of as-received Cu-1Cr-0.1Zr were as good as GlidCop's, however, the creep rates of Cu-1Cr-0.1Zr, AMZIRC, and Cu-0.9Cr dropped dramatically after the brazing heat treatment. The creep properties of NARloy-Z were relatively poor. Thus after brazing, GRCop-84 and GlidCop Al-15 had better creep properties than the other alloys. In the brazed condition, at a strain rate of 10^{-6} sec^{-1} the step loaded creep stress for GlidCop Al-15 was about 160 MPa; at these same conditions the creep stress was about 110 MPa for GRCop-84, and about 60 MPa for the other three alloys, including as-received NARloy-z.
Effects of Brazing	GRCop-84 and GlidCop Al-15 were not significantly affected by the simulated braze. AMZIRC, Cu-1Cr-0.1Zr, and Cu-0.9Cr lost their strength due to the braze, with strengths dropping by about 80% or more (yield strength loss was about 50% due to the braze in NARloy-Z).

Figure Captions

Fig. 1 Typical as-extruded GRCo-84 microstructures.

Fig. 2 AMZIRC longitudinal microstructures in the as-received condition; longitudinal/drawing direction is horizontal; dark spots are likely Cu_5Zr .

Fig. 3 AMZIRC longitudinal microstructures after the simulated brazing heat treatment at 935 °C; longitudinal/ drawing direction is horizontal.

Fig. 4 GlidCo Al-15 longitudinal micrograph of the as-received condition; longitudinal/drawing direction is horizontal.

Fig. 5 GlidCo Al-15 longitudinal microstructures after the simulated brazing heat treatment at 935 °C; longitudinal/drawing direction is horizontal.

Fig. 6 Cu-1Cr-0.1Zr micrograph of the as-received condition.

Fig. 7 Cu-1Cr-0.1Zr longitudinal microstructures after the simulated brazing heat treatment at 935 °C; longitudinal/drawing direction is horizontal.

Fig. 8 Cu-0.9Cr micrographs of the as-received condition.

Fig. 9 Cu-0.9Cr micrograph of the brazed condition.

Fig. 10 Ultimate tensile stress for as-received and brazed GRCo-84, AMZIRC, GlidCo Al-15, Cu-1Cr-0.1Zr, and Cu-0.9Cr alloys. GRCo-84 values are the average of HIPed and extruded material, data points represent averages of multiple tests, five tests at each temperature for GRCo-84, most others are the average of two tests. Average values for NARloy-Z taken from the literature are shown as a dashed line.^[9,14,15,21]

Fig. 11 Yield Strength, in units of MPa, at 0.2% off-set strain for as-received and brazed GRCo-84, AMZIRC, GlidCo Al-15, Cu-1Cr-0.1Zr, and Cu-0.9Cr alloys. GRCo-84 values are the average of HIPed and extruded material, data points represent averages of multiple tests, five tests at each temperature for GRCo-84, most others are the average of two tests. Average values for NARloy-Z taken from the literature are shown as dashed lines.^[9,14,15,21]

Fig. 12 Elongation in tensile of as-received and braze heat treated GRCo-84, AMZIRC, GlidCo Al-15, Cu-1Cr-0.1Zr, and Cu-0.9Cr alloys. Data points represent averages of multiple tests, five tests at each temperature for GRCo-84, most others are the average of two tests.

Fig. 13 Reduction in cross-sectional area for as-received and brazed GRCo-84, AMZIRC, GlidCo Al-15, Cu-1Cr-0.1Zr, Cu-0.9Cr alloys. GRCo-84 values are the average of HIPed and extruded material, data points represent averages of multiple tests, five tests at each temperature for GRCo-84, most others are the average of two tests.

Fig. 14 Compressive Yield Strength, defined as the compressive stress at 0.2% off-set strain, for GRCo-84, AMZIRC, GlidCo Al-15, Cu-1Cr-0.1Zr, and Cu-0.9Cr alloys at various test temperatures; data points are from averages of multiple tests, two or three tests at each temperature for each alloy.

Fig. 15 Step loaded creep rate data in the linear region of the log – log plot of strain rate and applied stress, with superimposed power function; power function constants are given in Table 9. All data at 500 °C are in black and use smaller symbols, data at 650 and 800 °C are gray or colored and use larger symbols.

Fig. 16 Constant load creep and resulting secondary creep strain rates with superimposed power law functions, power function constants shown in Table 11; data at 500 °C are black, larger like symbols are at the higher temperature. The GRCo-84 lines shown are from the power law creep rate equations presented in Table 11, from analysis of previous creep tests presented in Ref. 24. NARloy-Z data shown by dashed lines, and at 800 °C by a shaded line near the ordinate at 3×10^{-6} /sec, were taken from Ref. 23.

Fig. 17 Thermal Expansion results, lines are plots of equation (1) and the quadratics from Table 5.

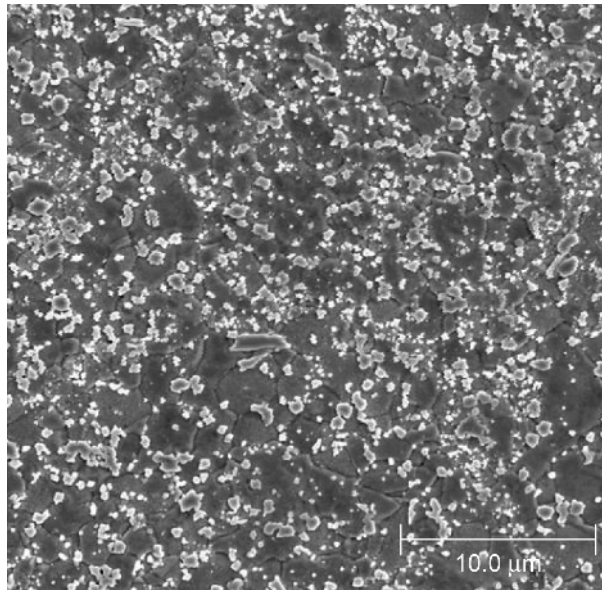


Figure 1

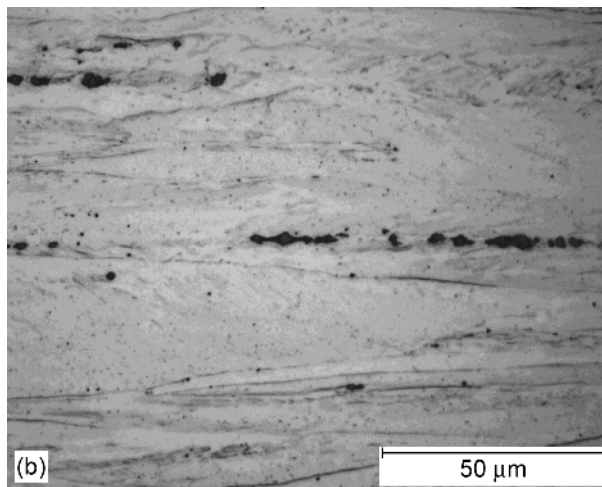
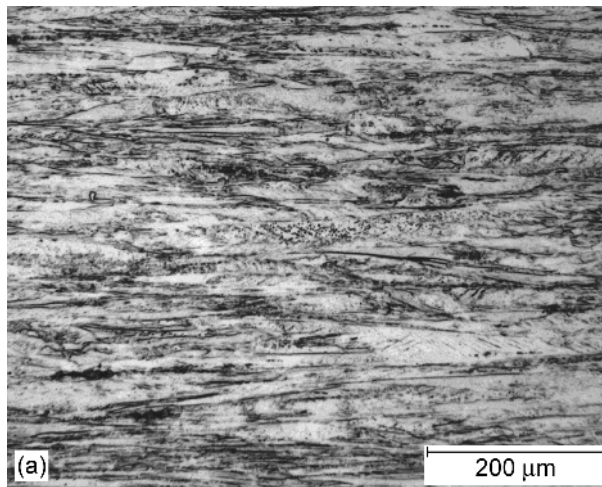


Figure 2

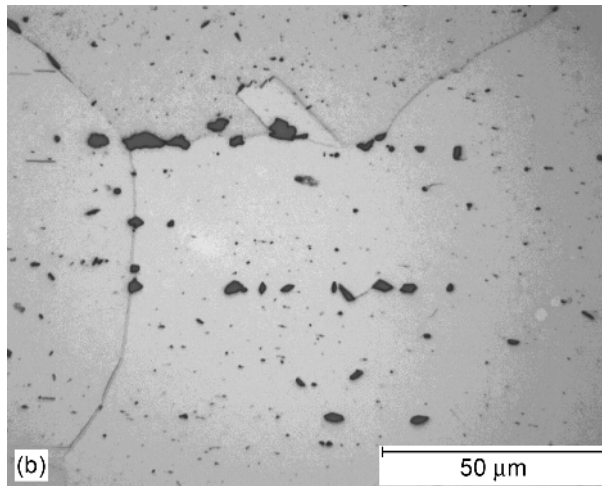
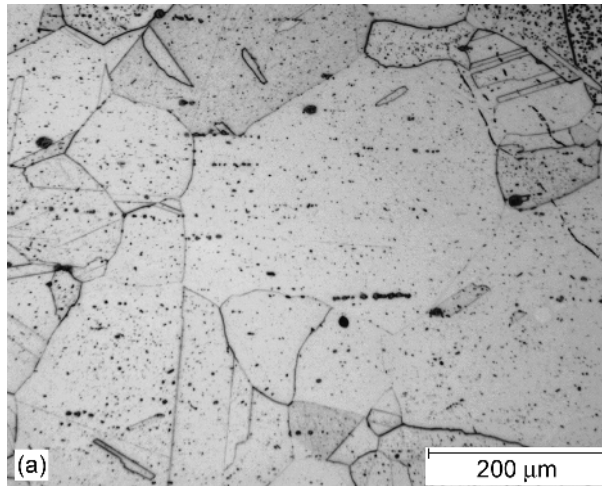


Figure 3

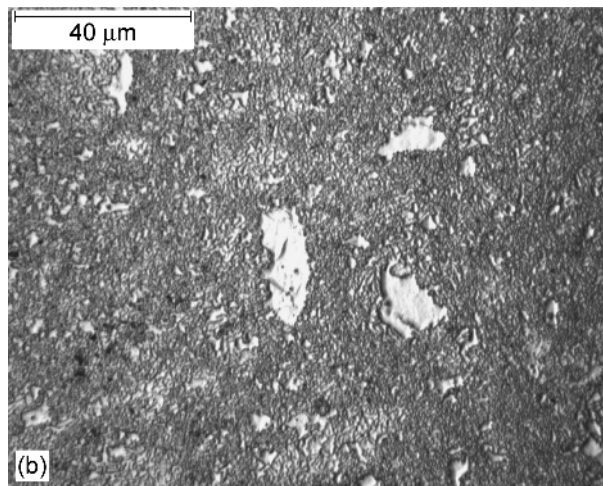
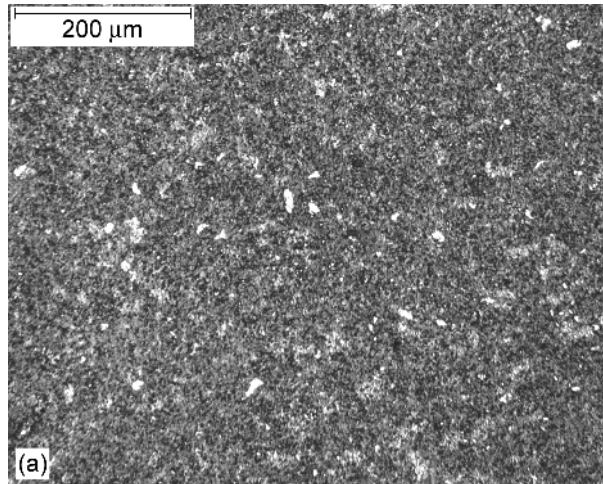


Figure 4

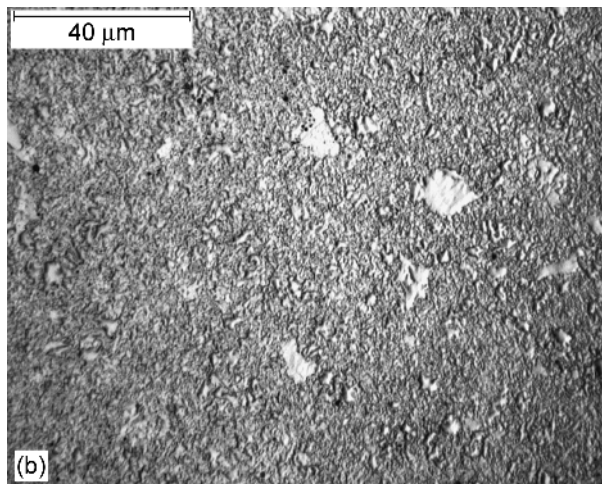
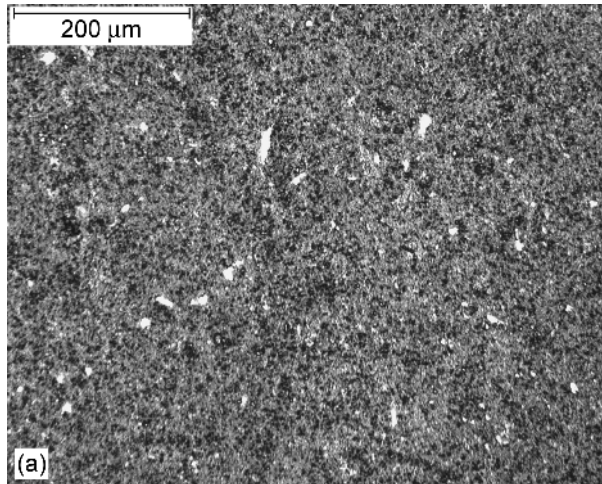


Figure 5

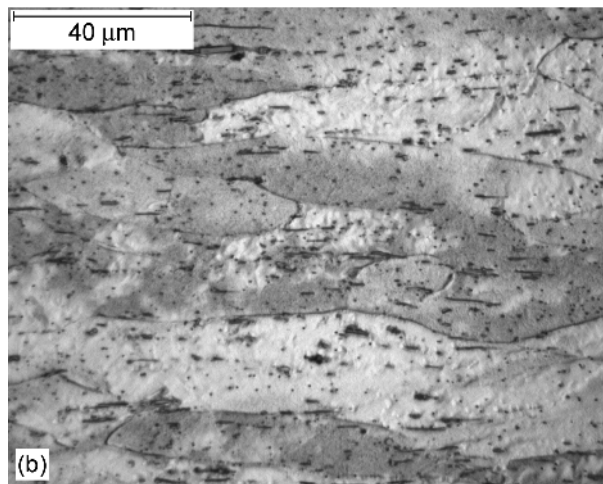
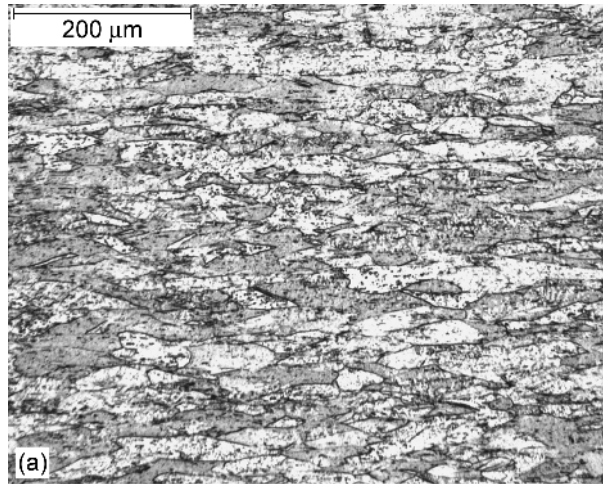


Figure 6

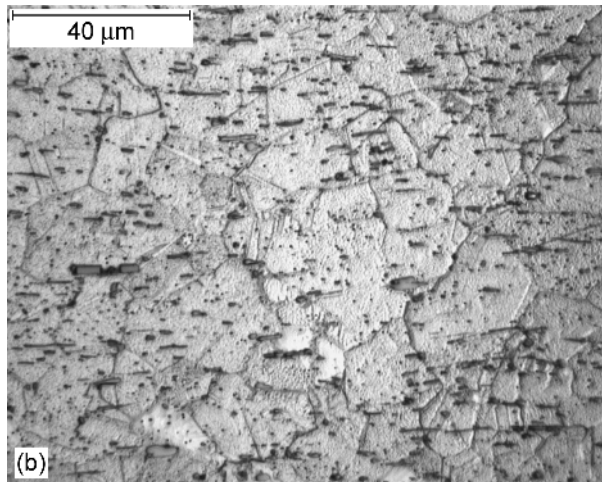
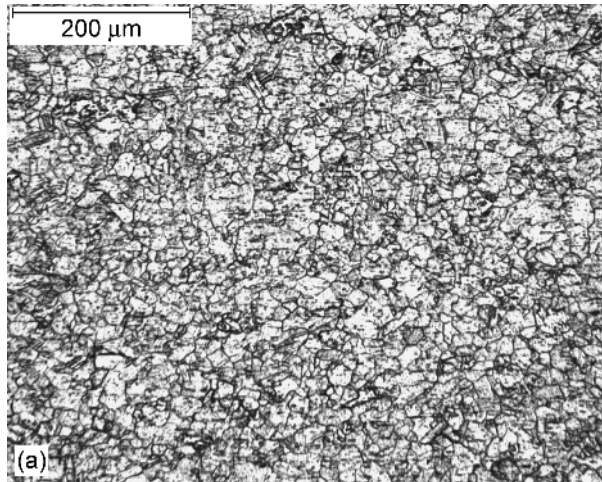


Figure 7

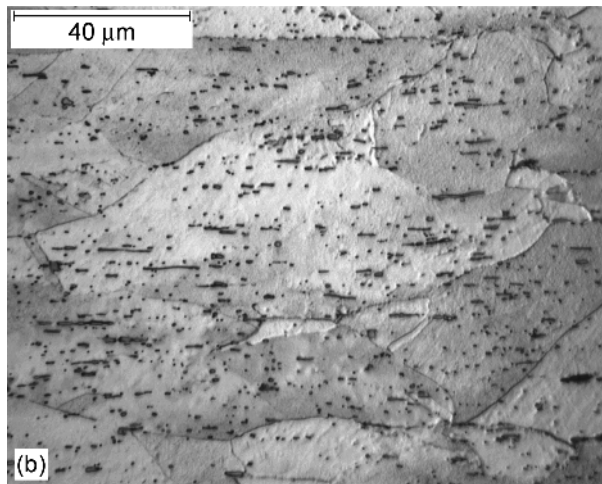
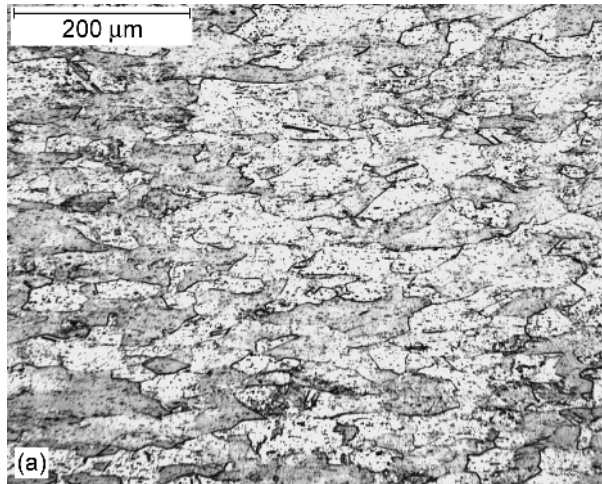


Figure 8

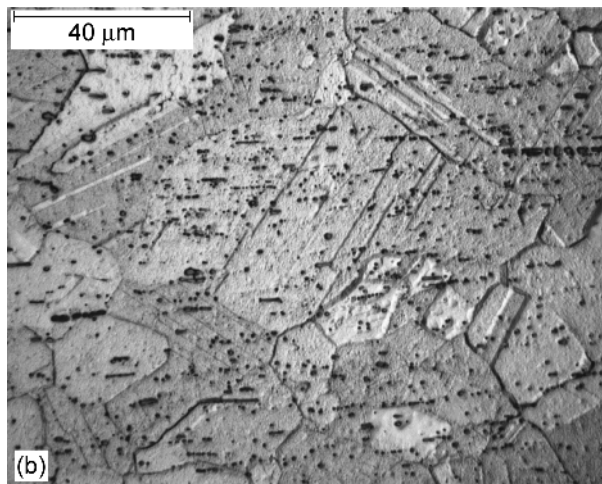
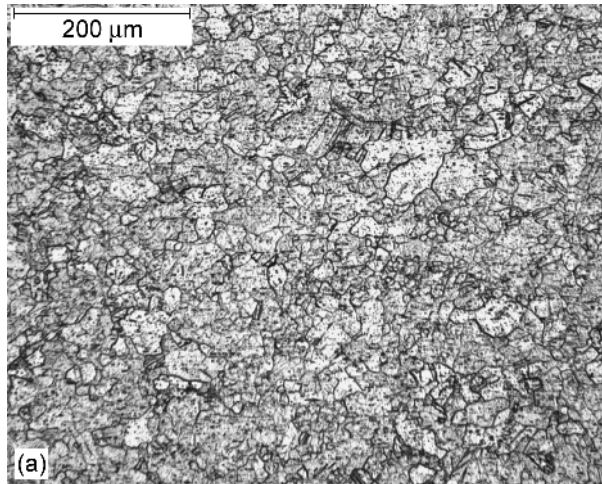


Figure 9

- GRCop-84, as-received
- GRCop-84, braze 935
- △— AMZIRC, as-received
- ▲— AMZIRC, braze 935
- GlidCop, as-received
- GlidCop, braze 935
- ◇— CuCrZr, as-received
- ◆— CuCrZr, braze 935
- CuCr, as-received
- ×— CuCr, braze 935
- ...— NARloy-Z, as-received
- - NARloy-Z, braze 935

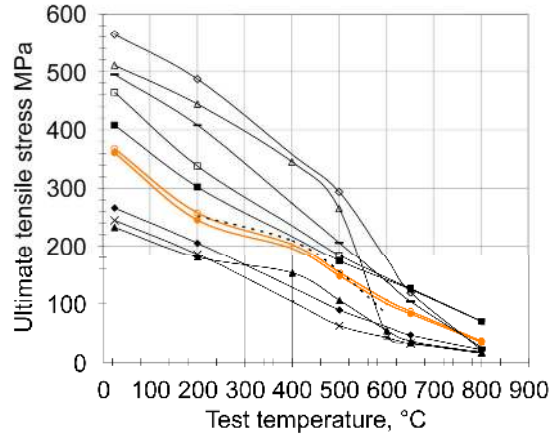


Figure 10

- GRCop-84, as-received
- GRCop-84, braze 935
- △— AMZIRC, as-received
- ▲— AMZIRC, braze 935
- GlidCop, as-received
- GlidCop, braze 935
- ◇— CuCrZr, as-received
- ◆— CuCrZr, braze 935
- CuCr, as-received
- ×— CuCr, braze 935
- ...— NARloy-Z, as-received
- - NARloy-Z, braze 935

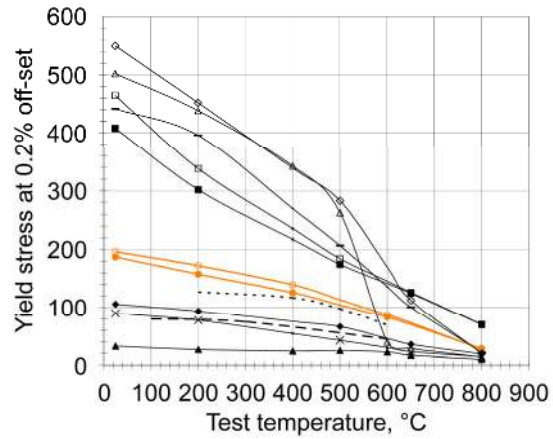


Figure 11

- GRCop-84, as-received
- GRCop-84, braze 935
- AMZIRC, as-received
- AMZIRC, braze 935
- GlidCop, Al-15, as-received
- GlidCop, Al-15, braze 935
- CuCrZr, as-received
- CuCrZr, braze 935
- CuCr, as-received
- CuCr, braze 935

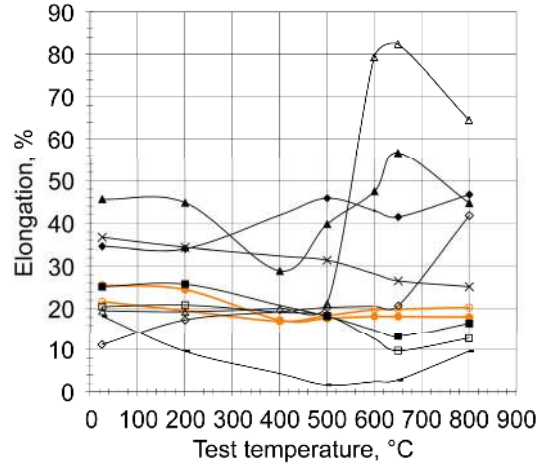


Figure 12

- GRCop-84, as-received
- GRCop-84, braze 935
- AMZIRC, as-received
- AMZIRC, braze 935
- GlidCop, Al-15, as-received
- GlidCop, Al-15, braze 935
- CuCrZr, as-received
- CuCrZr, braze 935
- CuCr, as-received
- CuCr, braze 935

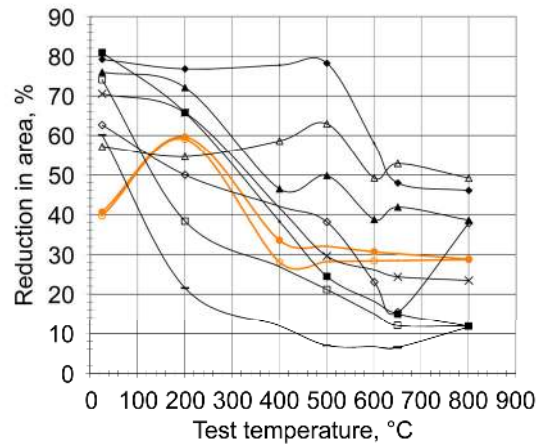


Figure 13

- GRCop-84, as-received
- AMZIRC, as-received
- AMZIRC, braze 935
- GlidCop, as-received
- GlidCop, braze 935
- CuCrZr, as-received
- CuCrZr, braze 935
- CuCr, as-received
- CuCr, braze 935

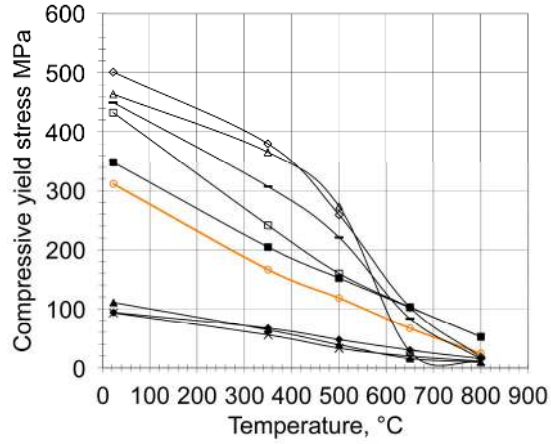


Figure 14

- GRCop-84, 500 °C
- GRCop-84, 650 °C
- GRCop-84, 800 °C
- △ AMZIRC, as-received, 500 °C
- ▲ AMZIRC, braze 935, 500 °C
- △ AMZIRC, as-received, 650 °C
- ▲ AMZIRC, braze 935, 650 °C
- GlidCop, as-received, 500 °C
- GlidCop, braze 935, 500 °C
- GlidCop, as-received, 650 °C
- GlidCop, braze 935, 650 °C
- CuCrZr, as-received, 500 °C
- CuCrZr, as-received, 650 °C
- ◆ CuCrZr, braze 935, 650 °C
- + CuCr, as-received, 500 °C
- x CuCr, braze 935, 500 °C
- + CuCr, as-received, 650 °C
- x CuCr, braze 935, 650 °C

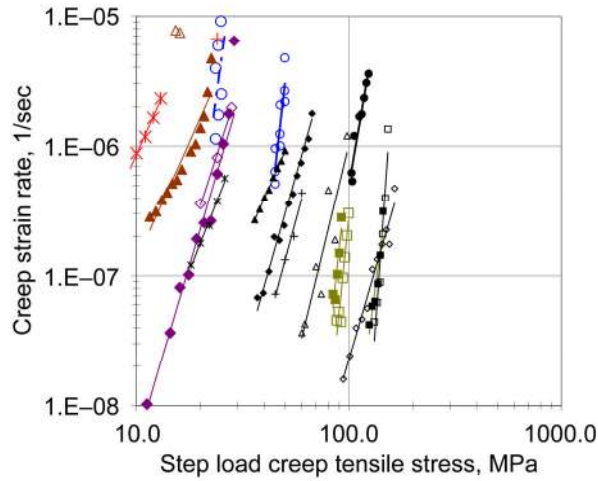


Figure 15

- GlidCop, as-received, 500 °C
- Rate equation
- GlidCop, brazed, 500 °C
- Rate equation
- GlidCop, as-received, 650 °C
- Rate equation
- GlidCop, brazed, 650 °C
- Rate equation
- ◇ CuCrZr, as-received, 500 °C
- Rate equation
- ◆ CuCrZr, brazed, 500 °C
- Rate equation
- ◇ CuCrZr, as-received, 650 °C
- Rate equation
- ◆ CuCrZr, brazed, 650 °C
- Rate equation
- △ AMZIRC, as-received, 500 °C
- Rate equation
- ▲ AMZIRC, brazed, 500 °C
- Rate equation
- △ AMZIRC, as-received, 650 °C
- Rate equation
- ▲ AMZIRC, brazed, 650 °C
- Rate equation
- + CuCr, as-received, 500 °C
- Rate equation
- * CuCr, brazed, 500 °C
- Rate equation
- * CuCr, brazed, 650 °C
- Rate equation
- GRCop-84, 500 °C
- Rate equation
- GRCop-84, 650 °C
- Rate equation
- GRCop-84, 800 °C
- Rate equation
- ⋯ NARloy-Z, as-received, 500 °C
- Rate equation
- ⋯ NARloy-Z, as-received, 650 °C
- Rate equation
- ⋯ NARloy-Z, as-received, 800 °C
- Rate equation

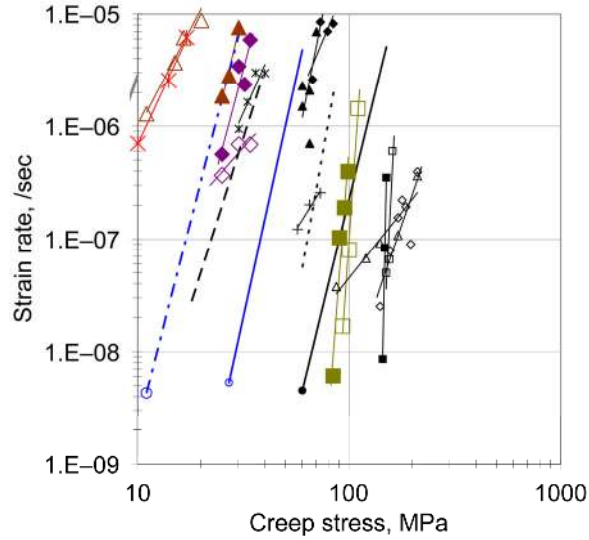


Figure 16

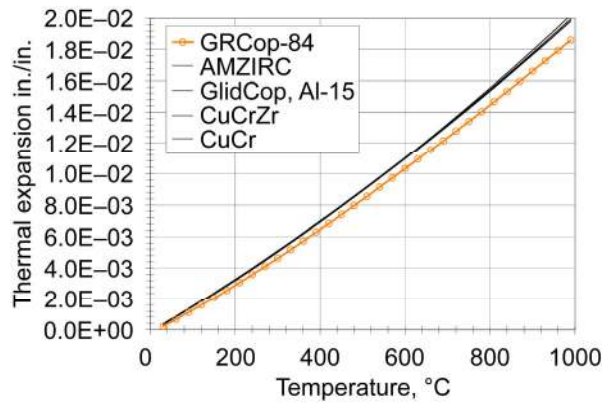


Figure 17